Supporting Information for "From Stream Flows to Cash Flows: Leveraging Evolutionary Multi-Objective Direct Policy Search to Manage Hydrologic Financial Risk"

Andrew L. Hamilton[1,2], Gregory W. Characklis[1,2], and Patrick M. Reed[3]

[1]Department of Environmental Sciences and Engineering, University of North Carolina at Chapel Hill, Chapel Hill, North Carolina, USA

[2]Center on Financial Risk in Environmental Systems, University of North Carolina at Chapel Hill, Chapel Hill, North Carolina, USA

[3]Department of Civil and Environmental Engineering, Cornell University, Ithaca, New York, USA

Contents of this file

Corresponding author: Andrew L. Hamilton, `andrew.hamilton@unc.edu`

Introduction

This Supporting Information (SI) provides additional methodological details related to the power price index (Section S1), in support of Section 2.2 of the main text. Additionally, this SI provides Table S1 (supporting Section 4.2 of the main text), Figure S1 (supporting Section 2.1 of the main text), Figure S3 (supporting Section 2.2 of the main text and Section S1 of SI), Figure S3 (supporting Section 2.2 of the main text), Figure S4 (supporting Section 4.2 of the main text), Figure S5 (supporting Section 5.2 of the main text), and Figures S6-S7 (supporting Section 5.3 of the main text).

S1: Power price index

The power price index (ε^P, in \$/MWh) is the third stochastic driver described in Section 2.2 of the main text. Like the other two drivers, ε^P is derived from the one million years of monthly synthetic hydro-financial records from Hamilton, Characklis, and Reed (2020); specifically, it is based on the monthly time series of wholesale power price and hydropower generation.

Let $\bar{G}_m$ be the average excess hydropower sold into the wholesale market in month m. This quantity is highest in the spring and early summer, when the alpine snow melts. It is lowest, and negative, during the autumn dry season, when hydropower is often insufficient to meet retail electricity demand. The generation-weighted average power price for water year t is defined as

$$P_t^{wt} = \frac{1}{12} \frac{\sum_{m=1}^{12} \bar{G}_m P_{m,t}}{\sum_{m=1}^{12} \bar{G}_m} \tag{1}$$

where $P_{m,t}$ is the power price in the mth month of water year t (\$/MWh). P_t^{wt} will be highest for years in which dry-season power prices are lower than average and wet-season power prices are higher than average, both of which are generally beneficial from a net revenue perspective.

The generation-weighted average power price over the coming year can be predicted via linear regression in log-space, using information about power prices from the prior year:

$$\ln P_t^{wt} = \hat{\beta}_0 + \hat{\beta}_1 \ln P_{t-1}^{wt} + \hat{\beta}_2 \ln P_{12,t-1} + \epsilon \tag{2}$$

where $P_{12,t-1}$ is the power price in September, the final month of the prior water year, $\hat{\beta}_i$ are the estimated regression coefficients, and ϵ is the regression residual, assumed to follow a normal distribution with mean 0 and standard deviation σ.

Now the power price index is defined as the expected value of the generation-weighted average power price over the coming water year, conditional on the information from the prior year.

$$\begin{aligned}
\varepsilon_t^P &= E[P_t^{wt} \mid P_{t-1}^{wt},\ P_{12,t-1}] && (3)\\
&= E\left[\exp(\hat{\beta}_0 + \hat{\beta}_1 \ln P_{t-1}^{wt} + \hat{\beta}_2 \ln P_{12,t-1} + \epsilon)\right] && (4)\\
&= \exp(\hat{\beta}_0) \cdot (P_{t-1}^{wt})^{\hat{\beta}_1} \cdot (P_{12,t-1})^{\hat{\beta}_2} \cdot E[\exp(\epsilon)] && (5)\\
&= \exp(\hat{\beta}_0) \cdot (P_{t-1}^{wt})^{\hat{\beta}_1} \cdot (P_{12,t-1})^{\hat{\beta}_2} \cdot \exp(\sigma^2/2) && (6)
\end{aligned}$$

where σ is the standard deviation of the normally-distributed residuals from the log-space regression.

This power price index (in units of \$/MWh) thus predicts the generation-weighted average power price over the coming water year, t, using the information available from the prior water year, $t-1$. The performance of this index can be assessed by plotting the power price index against the realized generation-weighted average power price (Figure S2). This relationship is found to have a correlation coefficient of 0.35.

Tables

Table S1. Parameters for multi-objective optimization with the Borg Multi-Objective Evolutionary Algorithm.

Parameter	Value
Number of samples per function evaluation	50,000
Number of function evaluations per Borg MOEA run	150,000
Number of seeds for Borg MOEA	30
Number of radial basis functions (M)	2
Number of informational inputs to policy (L)	4
ϵ-dominance parameter for J^{cash}	\$0.075 M/year
ϵ-dominance parameters for J^{debt}	\$0.225 M
ϵ-dominance parameter for J^{hedge}	\$0.05001
ϵ-dominance parameters for J^{fund}	\$0.225 M

Figures

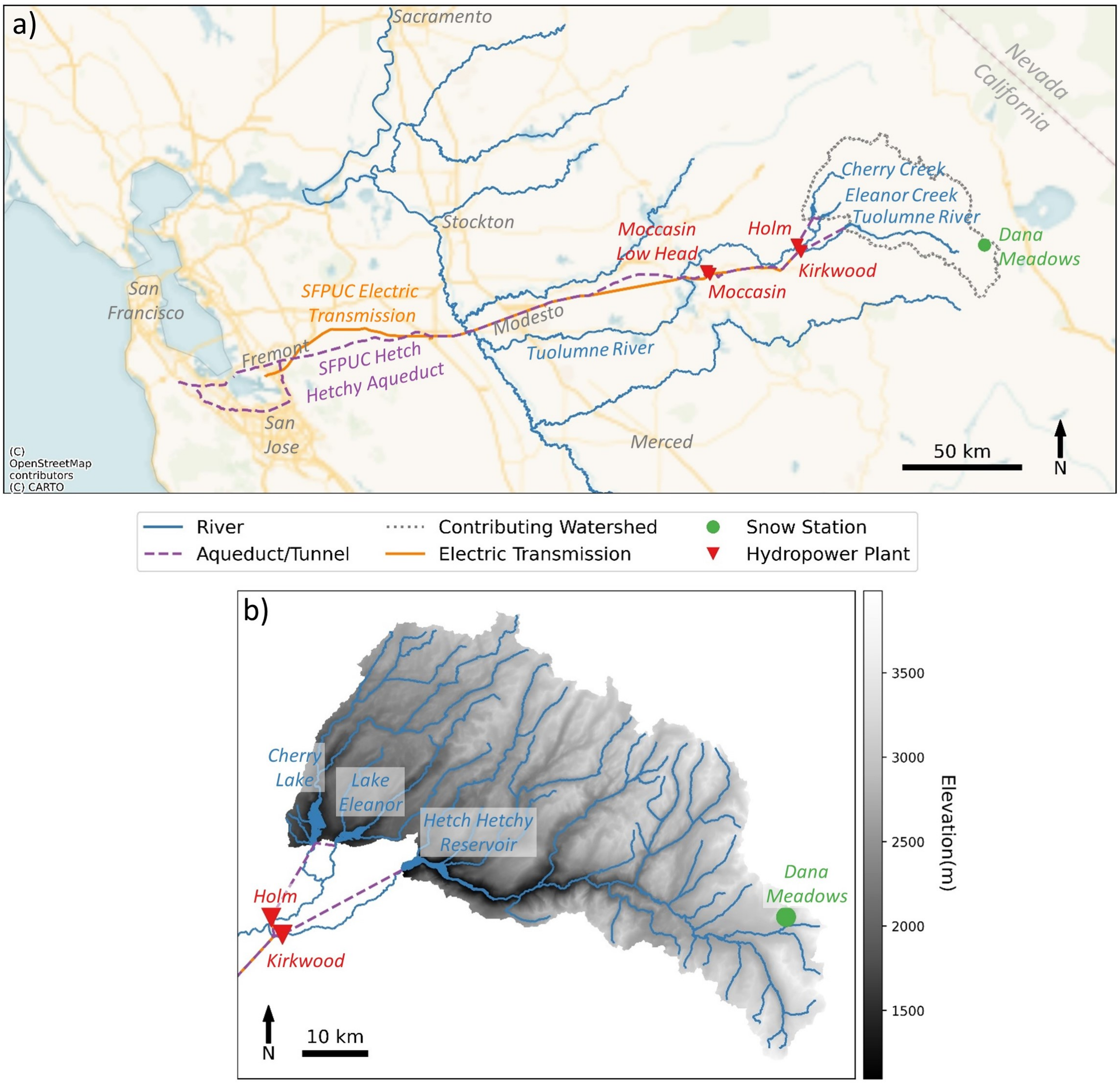

Figure S1. (a) Map of the study region. (b) Zoomed in map of the contributing watershed. Figure reproduced from Hamilton et al. (2020) Supporting Information.

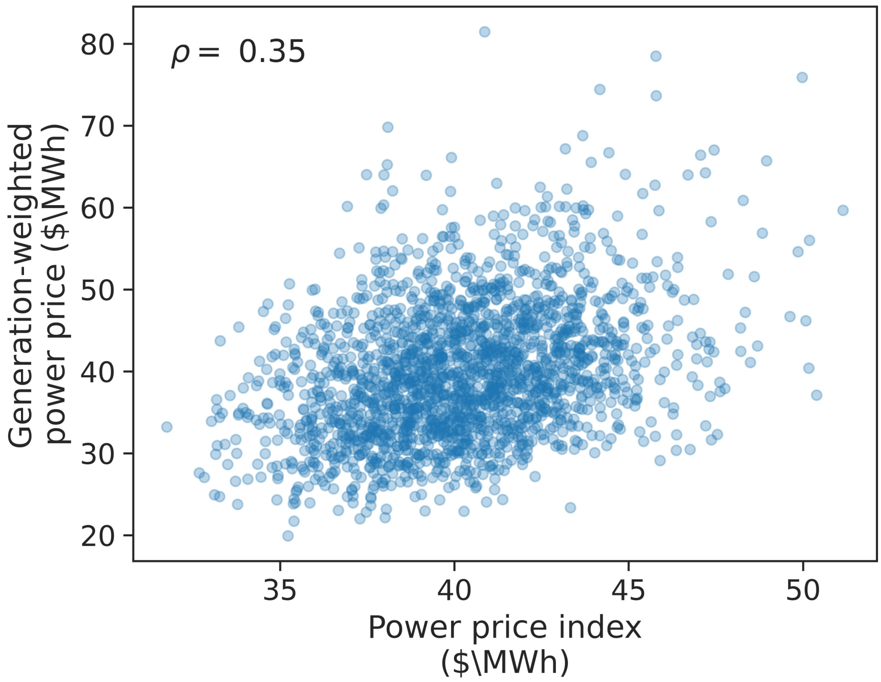

Figure S2. Relationship between power price index and generation-weighted average power price, along with correlation coefficient ρ. Only 2000 data points shown for clarity.

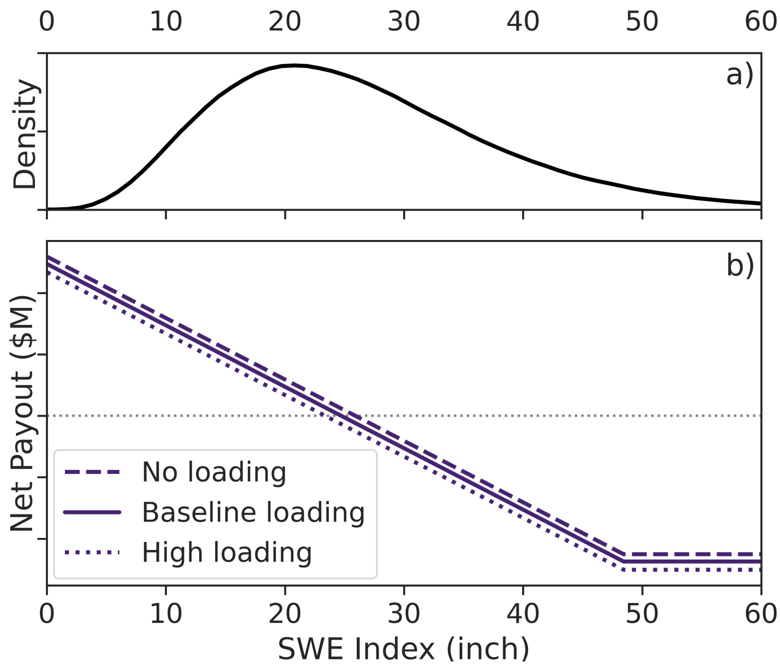

Figure S3. (a) Probability density for SWE index, a weighted average of February 1 and April 1 observations. (b) Net payout function for the capped contract for differences (CFD). The threshold separating positive and negative payouts is 24.71 inches. The slope of this contract is controlled by either the static or dynamic control policy. Present study uses the "baseline" loading. Figure adapted from Hamilton et al. (2020).

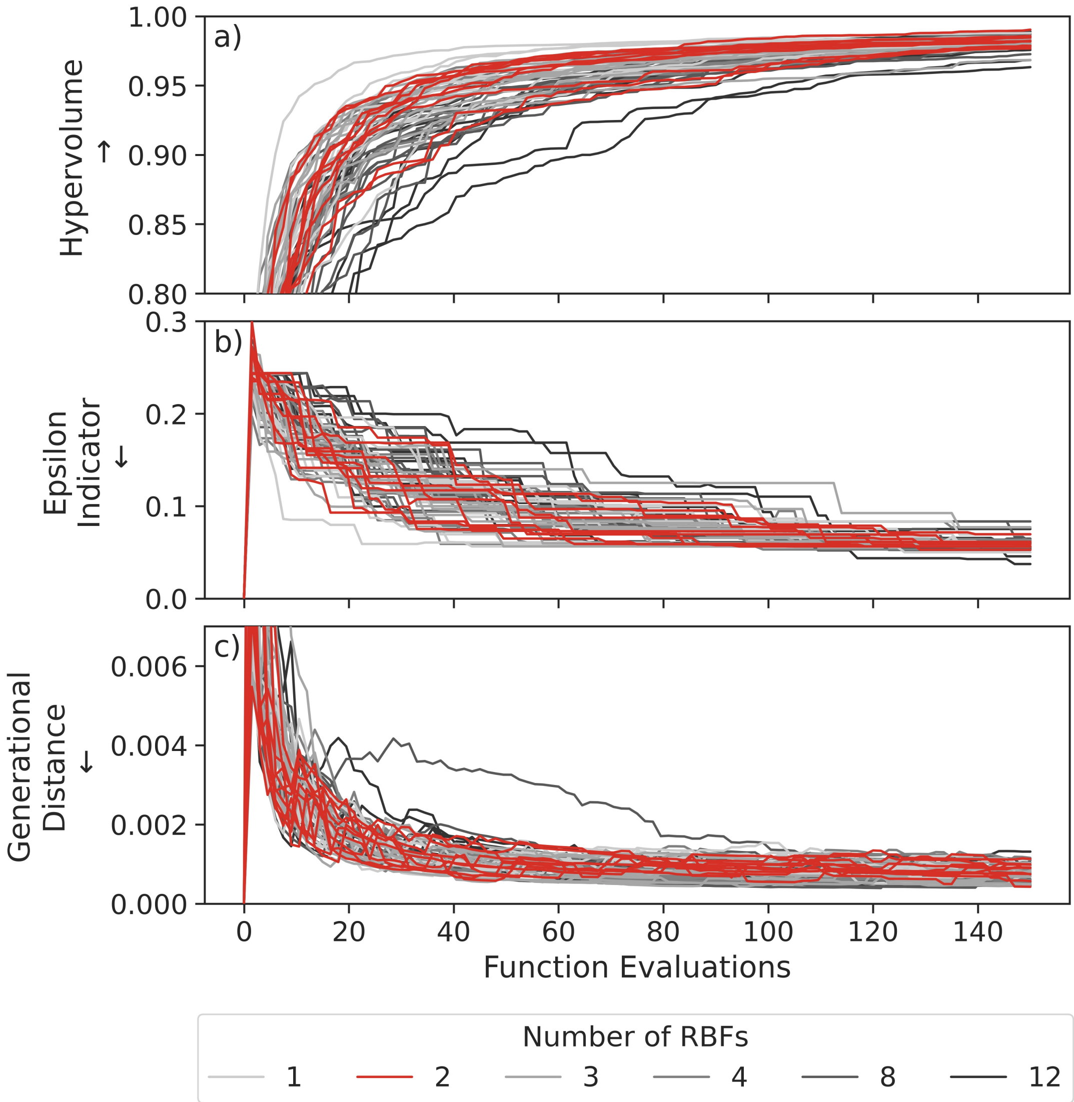

Figure S4. Convergence metrics for approximate Pareto sets from the Borg MOEA, using different numbers of radial basis functions (RBFs), for 10 random seeds each: (a) Hypervolume metric; (b) Generational distance metric; (c) Additive epsilon indicator metric.

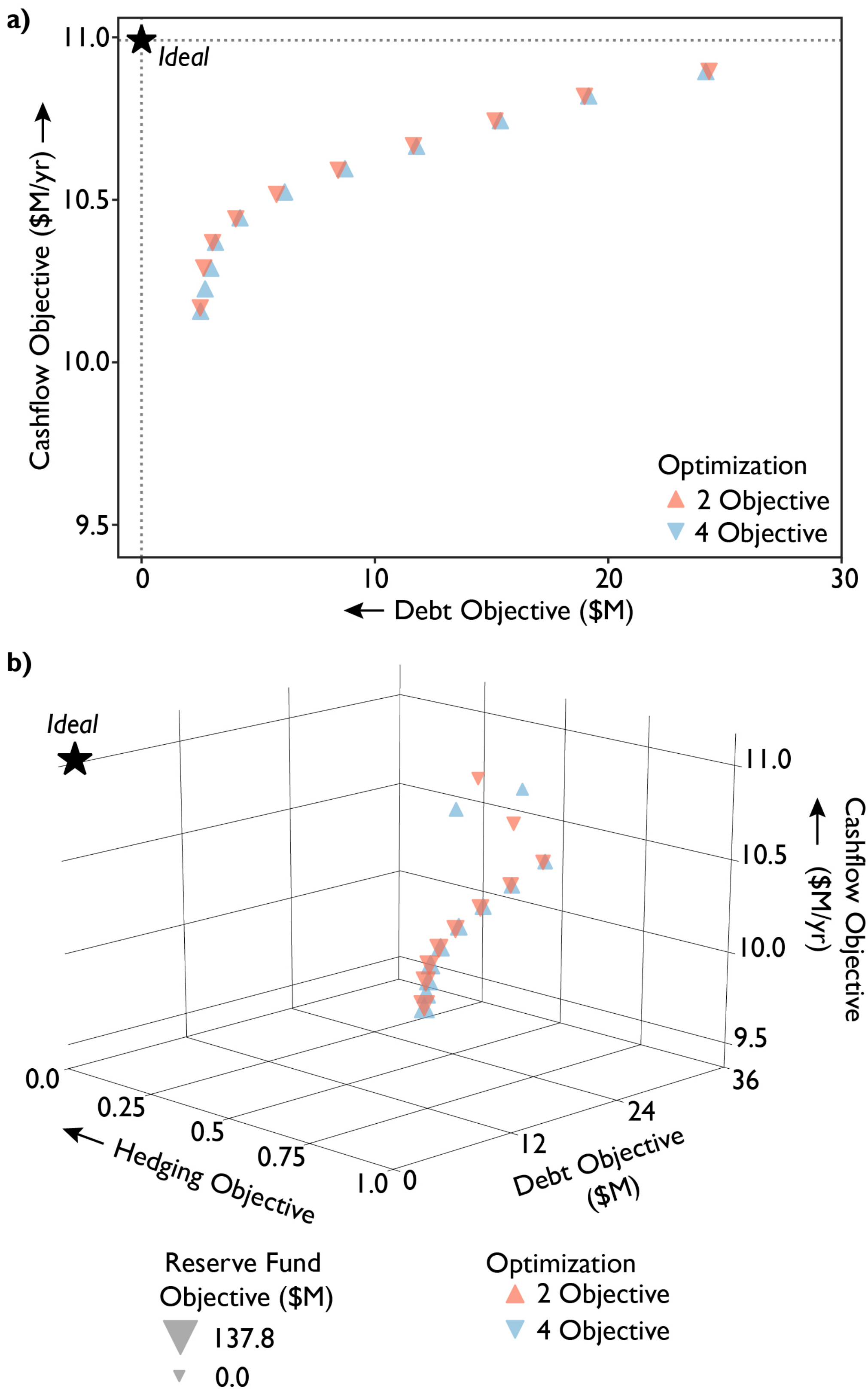

Figure S5. Results from 2-objective and 4-objective optimization problems, after filtering for non-dominated solutions with respect to the 2-objective problem (J^{cash} vs. J^{debt}). Results displayed for both 2-objective (a) and 4-objective (b) performance.

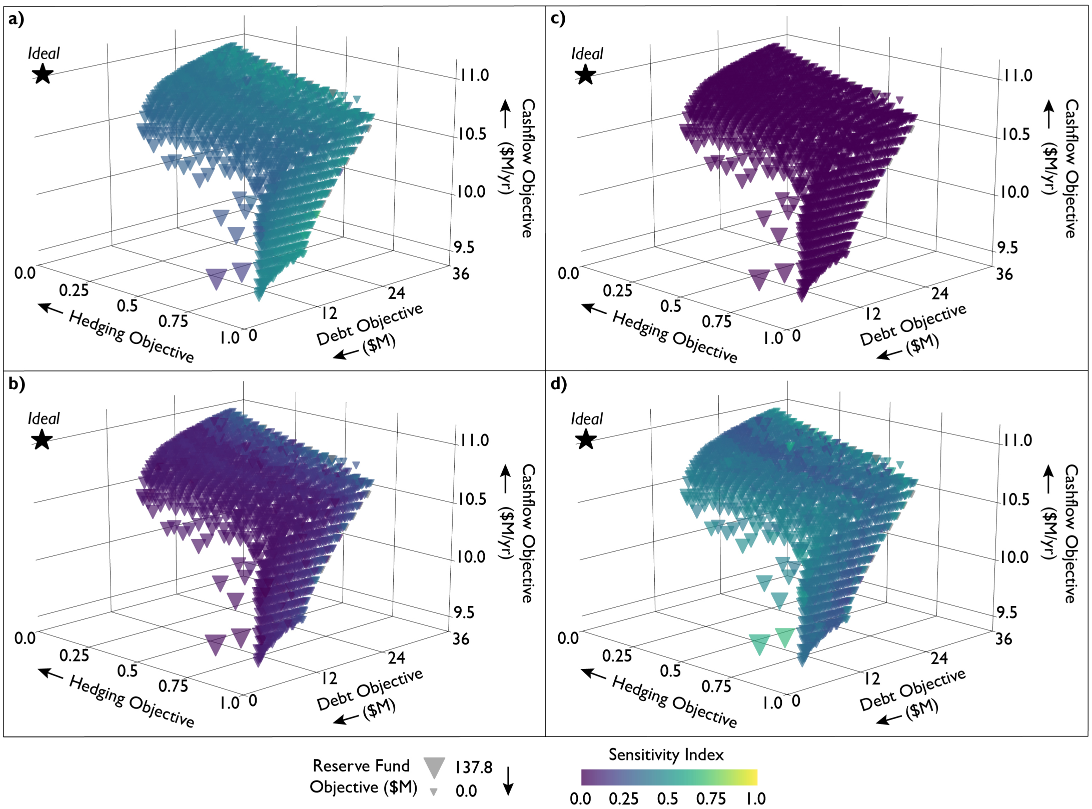

Figure S6. Entropic sensitivity indices, relative to withdrawal/deposit decision, for the reserve fund balance (a), debt (b), power price index (c), and incoming cash flow (Cash Flow 2) (d).

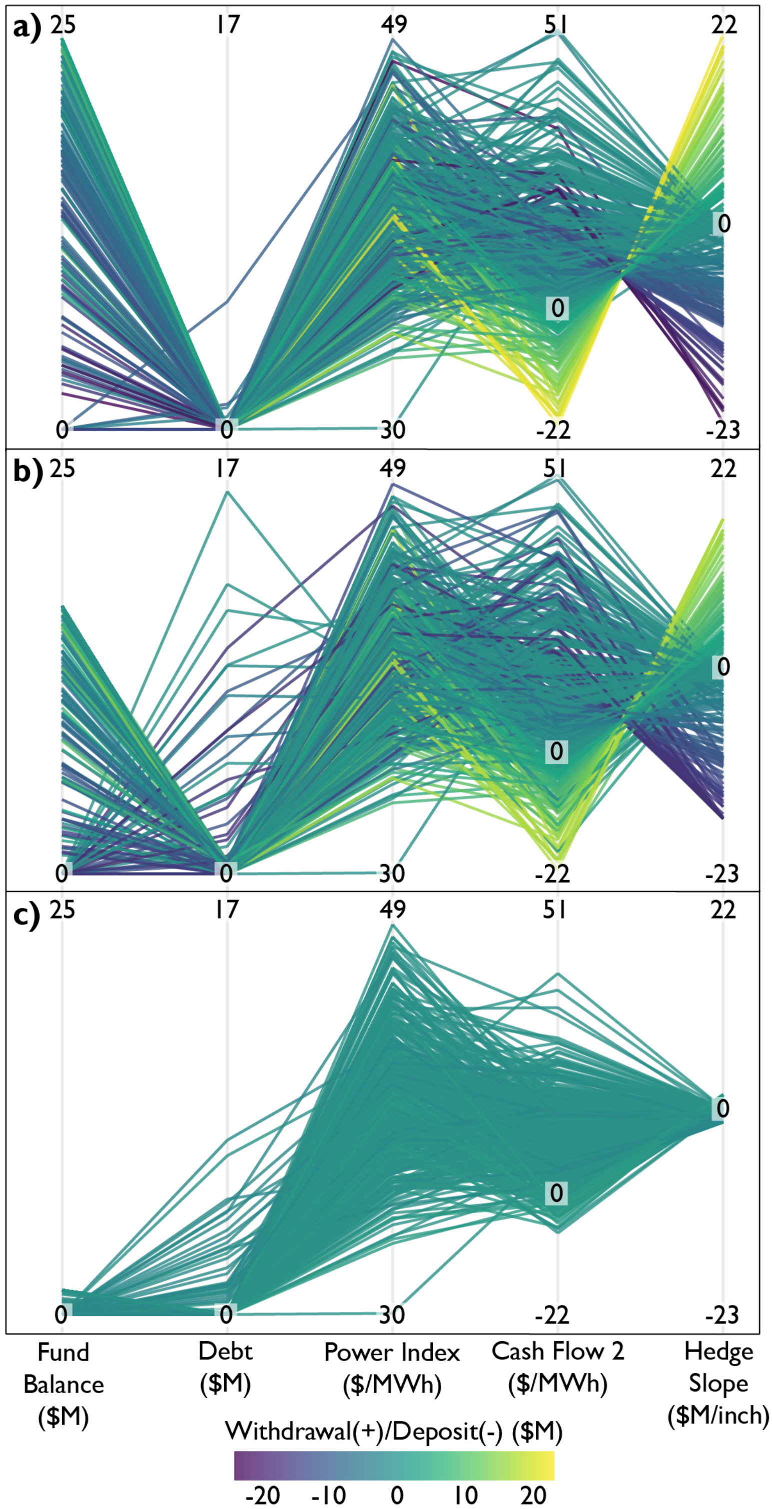

Figure S7. Withdrawal/Deposit control policy visualization for three chosen policies in Figure 8 and rows 4-6 of Table 2 in the main text. The policies are chosen due to their high sensitivity (with respect to the hedging control policy) to the reserve fund (a), debt (b), and power price index (c) information.

References

Hamilton, A. L., Characklis, G. W., & Reed, P. M. (2020). Managing financial risk tradeoffs for hydropower generation using snowpack-based index contracts. *Water Resources Research*, *56*, e2020WR027212. doi: 10.1029/2020wr027212